

## Investigation of methods of reducing the number of pinhole defects in glossy-opaque floor tile glaze by modifying glaze properties

Ayşe Tunali\*

Eczacıbaşı Building Product Co.- Vitra R&D Center-(Vitra Innovation Center)

Improvement of surface quality of glossy-opaque floor tile glazes by decreasing pinhole problem was the main purpose of this study. Glossy-opaque floor tile glaze was produced by mixing three different frit compositions. Effects of frit compositions on glaze surface properties were investigated by thermal analysis. Two hypotheses were improved and applied in terms of the analysis results. It was found that pinhole problems can be solved by optimizing softening point of glaze composition and glossy-opaque glaze with enhanced functional and aesthetic features can be obtained by homogeneously distributed nano size crystals.

**Key words:** Glass-ceramic, Porosity, Optical properties, Microstructure-final, Functional application

### Introduction

The optical characteristics of glazes, glasses and enamels perceived by an observer are the result of light reflection and scattering, caused by small particles or discontinuous nuclei in their interior [1]. The most important optical characteristics are those related to the amount (percentage) of specular reflection (which determines brightness) and the amount of transmitted light (which determines colour, depth, saturation, etc.), as a function of the fraction of diffusely transmitted light.

The opacity and covering characteristics of glasses and glazes depend on the amount of diffuse light reflected by top surface, before reaching the bottom surface [2]. The opacity power depends on light scattering by particles or nuclei present in the binary system, directly related to size, form, concentration and refractive index of the secondary phase [3-5]. Thus maximum light scattering occurs, or in other terms, to maximize the diffuse reflection, secondary phase particles must have a sufficiently different refractive index related to the matrix, and must have a particle size similar to the wavelength of the incident light. Second phase concentration must be relatively high; in order to present a high number of diffuse reflectance points [2].

Opaque glazes are used to cover unwanted body color and in the situations where aesthetics is important [3]. In the traditional opaque glazes used in floor tile industry, opacity usually originates through hardening of glass matrix by addition of a high amount of opacifiers, e.g. zircon, into the batch [6]. Nowadays the most

researches attend to improve the quality of glazes by development of new glaze products with more smooth, glossy surfaces and desirable mechanical and chemical properties at the similar firing conditions [6-8]. Glossiness has been found to be most closely related to the sharpness and perfection of the reflected image, and thus to the intensity of the specular reflection. The factors that affect the intensity of specular reflectance include the surface smoothness, the presence in the glaze of internal surfaces caused by crystals or phase separation, and the refractive index of the glaze [5].

It is rather difficult to control the process of sintering and devitrification of the glass-ceramic composition in the conventional firing cycle so that the surface of the glaze can be given both a gloss and an opaque appearance with no defect [9]. In a single firing process through which green ceramic body is fired, there occur a number of solid-gas reactions by which the clay and calcium present in the body get separated and organic substances get burned. These reactions should be completed before melting frit particles can cover the surface of the body. Otherwise, the resulting gas disrupts the quality of the surface of glaze by causing a pinhole defect while passing through the fused layer [10-11]. Similarly some surface defects (puncturing, pockets, etc) are caused by bubbles in the glaze which rise to the surface during the firing process, remaining there subsequently following the product cooling phase [10].

In the present study, despite having a gloss-opaque appearance, the R glaze with a pinhole defect over its surface, as well as the three different frits making up the glaze, has been investigated. By combining the data obtained by two thermal analytical techniques commonly used in the traditional ceramic field; i.e., differential thermal analysis (DTA) and heating microscope analysis (HeMA) sintering and devitrification properties of frits,

\*Corresponding author:  
Tel : +90-228-314-04-00  
Fax: +90-228-314-04-12  
E-mail: ayse.tunali@eczacibasi.com.tr

as well as of the glaze, were evaluated. The properties added to the glaze with the help of the frit components involved in the composition of the glaze were first evaluated. Then, a new glaze composition was developed by altering the ratios of the frit in such a way that would yield a perfect surface for the purpose that the chances for a defect could be reduced.

### Experimental Procedure

The industrially produced and used glaze (R) is composed of a mixture of A, B and C frits. Compositions of frits are given in Table 1. To understand the properties achieved by adding frits, each of the frits was prepared as a glaze. Then glaze R was prepared by mixing frit A, B and C. Table 2 shows the ratio of frits used to prepare glaze R and as well as the other glazes prepared individually by using only one kind of the frits.

To prepare these glazes, frits and kaolin were used. Carboxyl methyl cellulose and sodiumtripolyphosphate (STPP) were employed to improve glaze slip properties. The glazes were prepared under laboratory working conditions and applied on engobed green commercially available floor tile bodies made by Vitra Tile Cooperation. The dried samples were heat-treated according to fast-firing procedure used at Vitra Tile Company, maximum sintering temperature is 1180 °C and firing time is 32 minutes.

The characteristic glass transition temperature ( $T_g$ ), crystallization temperature ( $T_c$ ) and melting temperature ( $T_m$ ) were observed using a Netzsch STA 409 PG differential thermal analysis (DTA) using frit powders ground to < 63  $\mu\text{m}$  grain size. The heat treatment was

**Table 1.** Compositions of the industrially used frits A, B and C.

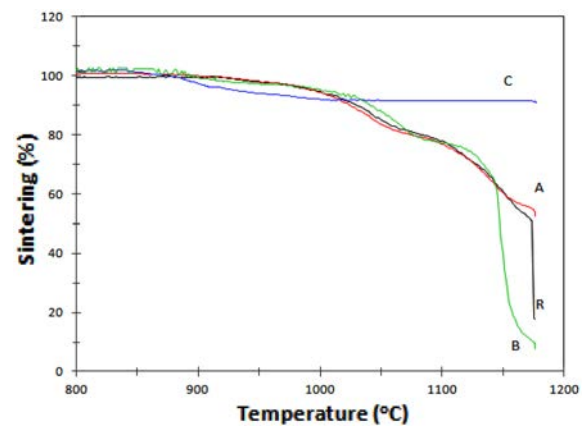
| Component  | Content (mol %) for frit A | Content (mol %) for frit B | Content (mol %) for frit C |
|--|----------------------------|----------------------------|----------------------------|
| R <sub>2</sub> O (Na <sub>2</sub> O, K <sub>2</sub> O)                             | 2,64                       | 3,84                       | 0,81                       |
| RO (CaO, MgO, ZnO)   | 26,15                      | 23,36                      | 38,47                      |
| R <sub>2</sub> O (B <sub>2</sub> O <sub>3</sub> , Al <sub>2</sub> O <sub>3</sub> ) | 6,1                        | 5,16                       | 3,99                       |
| RO <sub>2</sub> (SiO <sub>2</sub> , ZrO <sub>2</sub> )                             | 65,11                      | 67,64                      | 56,73                      |
| Total  | 100                        | 100                        | 100                        |

**Table 2.** Chemical analyses of the prepared glaze compositions (parts by weight).

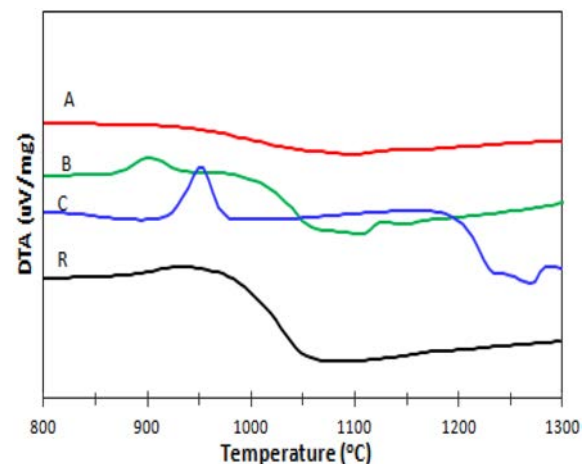
| Glaze   | Frit A | Frit B | Frit C | Kaolin |
|---------|--------|--------|--------|--------|
| Glaze R | 70,5   | 10     | 11     | 8,5    |
| Glaze A | 90     | –      | –      | 10     |
| Glaze B | –      | 90     | –      | 10     |
| Glaze C | –      | –      | 90     | 10     |

carried out in a platinum crucible by heating the sample from room temperature to the 1300 °C at a rate of 10 °C min<sup>-1</sup>. Data for the run were collected directly from the DTA. Samples were heated in a dilatometer (Netzsch DIL 402 PC) at a rate of 10 °C/min up to 1000 °C in order to determine glass transition temperature ( $T_g$  DIL), softening temperature ( $T_{sof}$  DIL) and thermal expansion coefficient values. The sintering behaviour was investigated by hot stage microscope (HSM) (Misura 3.32 ODHT-HSM 1600/80) measuring linear shrinkage in an industrial-like cycle. The colour values  $L^*$ ,  $a^*$  and  $b^*$  of all fired tiles were measured using a Minolta CR-300 series chroma meter. Gloss was determined in a reflectometer; using a 40°, 60° and 80° light incident angle on the glaze surface. A minimum of three measurements was run, which were subsequently averaged.

For evaluation of crystalline phases which were developed in glazes during heat-treatment, X-ray diffractometer (Rigaku Rint 2000 series) with Cu K $\alpha$  radiation was used. XRD patterns were taken from the fired glazed tile surfaces to identify the crystalline phases formed, working at 40 KV and 30 mA, with the scanning velocity of 2°/min. In order to study the effect of glaze composition on the formation, size and



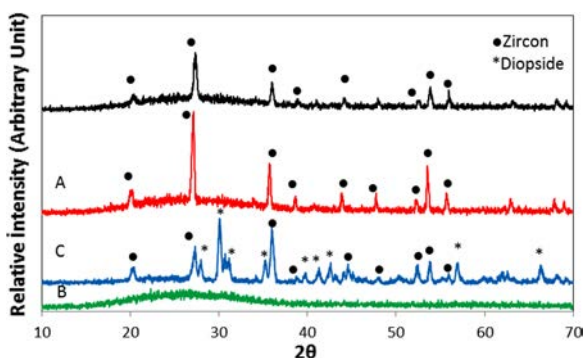
**Fig. 1.** Sintering behaviour of glazes R, A, B and C.



**Fig. 2.** DTA curves of glazes R, A, B and C.

**Table 3.** The characteristic temperature of glazes obtained from dilatometer, HSM and DTA analyses.

| Glaze   | Thermal expansion coefficient (DIL) (A400 × 10 <sup>-7</sup> ) | T <sub>g</sub> (DIL) (°C) | T <sub>softening</sub> (DIL) (°C) | T <sub>c</sub> (DTA) (°C) | T <sub>sintering</sub> (HSM) (°C) | T <sub>softening</sub> (HSM) (°C) | T <sub>sphere</sub> (HSM) (°C) | T <sub>half sphere</sub> | T <sub>melting</sub> |
|---------|--|---------------------------|-----------------------------------|---------------------------|-----------------------------------|-----------------------------------|--------------------------------|--------------------------|----------------------|
| Glaze R | 62,4   | 668                       | 816                               | 940                       | 1000                              | 1139                              | –                              | 1176                     | 1177                 |
| Glaze A | 57,1   | 670                       | 818                               | 900                       | 993                               | 1097                              | 1160                           | 1175                     | –                    |
| Glaze B | 64,5   | 677                       | 858                               | 902                       | 1002                              | 1127                              | –                              | –                        | 1175                 |
| Glaze C | 74,0   | 660                       | > 1000                            | 950                       | 928                               | –                                 | –                              | –                        | –                    |

**Fig. 3.** XRD pattern of glazes R, A, B and C fired at 1180 °C for 38 min.

distribution of the opacifying crystal phases, the samples analyzed with XRD were subjected to SEM (SUPRA-Zeiss-50) attached with an energy dispersive (EDX) spectrometer.

## Results and Discussion

Fig. 1 and Fig. 2 show the sintering curves and DTA curves of the above mentioned glazes, respectively. The characteristic temperature of glazes obtained from dilatometer, HSM (Fig. 1) and DTA (Fig. 2) analyses are given in Table 3. As was expected, frit A that makes up a large portion of the glaze had an effect on the characteristics of the glaze R.

Fig. 3 shows the X ray diffraction patterns of heat treated glazes. In the DTA curve (Fig. 2), we can see a broad peak for glaze A between 800 and 1000 °C, and this peak corresponds to zircon crystallization in Fig. 3.

Although glaze B has a completely amorphous structure (Fig. 3), an exothermic peak was observed around 900 °C in the DTA curve (Fig. 2). It was concluded that crystallization must have occurred in glaze B initially but these crystals are thought to have melted afterwards around 1050 °C within the amorphous matrix. Due to absence of crystals that could prevent a viscous flow in the structure, the system was determined to have been sintered rapidly in high temperatures varying between 1140 and 1180 °C (Fig. 1). When compared to the other frits, frit C had almost no signs of sintering in Fig. 1. Therefore, we concluded that the sharp peak in the DTA curve was suggestive of a dense crystallization, which must have prevented a viscous

**Table 4.** Chemical analyses of the prepared glazed compositions (parts by weight).

| Glaze | Frit A | Frit B | Frit C | Kaolin |
|-------|--------|--------|--------|--------|
| R     | 70,5   | 10     | 11     | 8,5    |
| R20A  | 73,4   | 9,1    | 9,9    | 7,6    |
| R50B  | 66,9   | 14,5   | 10,5   | 8,1    |
| R50C  | 66,7   | 9,6    | 15,7   | 8      |

flow. This, in turn, must have stopped sintering once the temperature rose over 1000 °C. The resulting crystals were determined to be zircon and diopside through an XRD analysis (Fig 3).

According to analyses of the three frits making up glaze R, zircon crystallization occurs in frit A in a wide range of temperature (Fig. 2 and Fig. 3). However, the process of crystallization affects its sintering in a negative way. When compared to the others, this frit has the lowest temperature for softening in Table 3 (T<sub>sof</sub> DIL and T<sub>sof</sub> HSM). The most important feature of frit B is that it can be sintered rapidly around 1150 °C (Fig. 1). As for frit C, even though this is the one with the lowest glass-transition temperature and has an early sintering temperature (Table 3), it fails to achieve a complete sintering because of zircon and diopside crystallization that occur in high levels in low temperatures (Fig. 1 and Fig. 3). In glaze C, both zircon and diopside occurred. Even though frit C was added to glaze R, only zircon could be crystallized within the system. Glaze R, which is composed of the aforementioned properties, turns out to suffer a pinhole problem over its surface.

We anticipate that two different methods could solve the problem of air bubbles coming to the surface of the glaze out of the body or of the engobe or the air bubbles resulting from low viscosity. Based upon this anticipation, new prescriptions have been devised. Our first anticipation is that additional time could be given to the system with a rise provided in the amount of the targeted crystal, thus increasing the softening point of the glaze. For this purpose, the amount of frit C in the glaze was increased. This prescription of glaze was codified as R50C. Our second anticipation is that gases could be trapped in the system and so be prevented from going up to the surface. Sintering and softening temperature could be lowered, and so the system could be sintered before gaseous bubbles can reach the

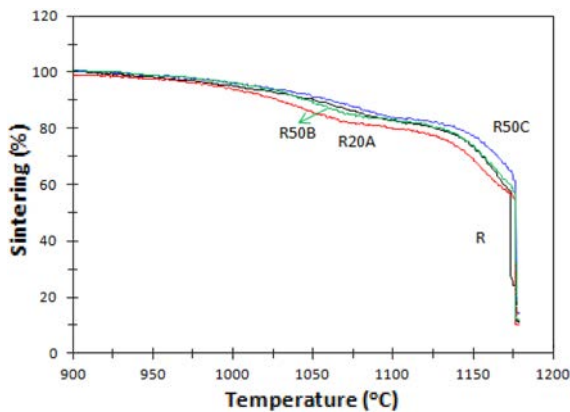


Fig. 4. Sintering behaviours of glazes R, R20A, R50B and R50C.

Table 5. The characteristic temperature obtained from sintering curves of glazes.

| Glaze | T <sub>sintering</sub> (°C) | T <sub>softening</sub> (°C) | T <sub>sphere</sub> (°C) | T <sub>half sphere</sub> (°C) |
|-------|-----------------------------|-----------------------------|--------------------------|-------------------------------|
| R     | 1000                        | 1139                        | –                        | 1176                          |
| R20A  | 992                         | 1127                        | 1160                     | 1176                          |
| R50B  | 1009                        | 1134                        | 1176                     | 1176                          |
| R50C  | 1015                        | 1146                        | 1175                     | 1176                          |

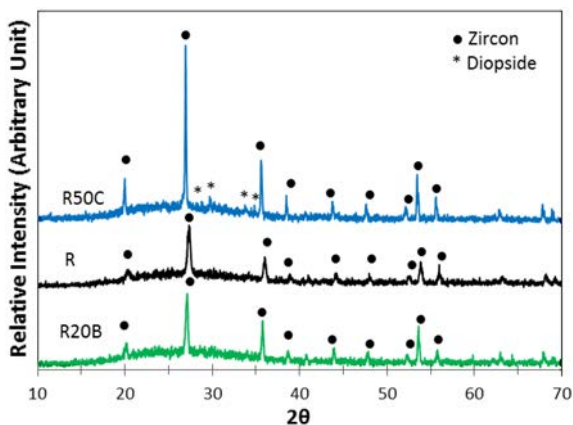


Fig. 5. XRD patterns of glazes R, R50C and R20B fired at 1180 °C for 38 min.

surface. For this purpose, the weight of frit A, whose sintering and softening temperatures are the lowest, was increased, thus creating a glaze prescription named R20A. Another purpose was to enable a very good sintering of the R50B glaze by increasing frit B. Because gas bubbles trapped in the glaze are likely to affect its mechanical properties, realization of the first anticipation appears to be of more significance. A comparison of frit ratios of the glazes prepared with the glaze R has been given in Table 4. All the glazes have been prepared and applied under the same conditions in consideration of an industrial scale.

Fig. 4 shows sintering curves of glazes, while Table 5 summarizes the results obtained from the sintering curve. As far as the first anticipation is concerned, the softening value of the R50C glaze, into which a lot more

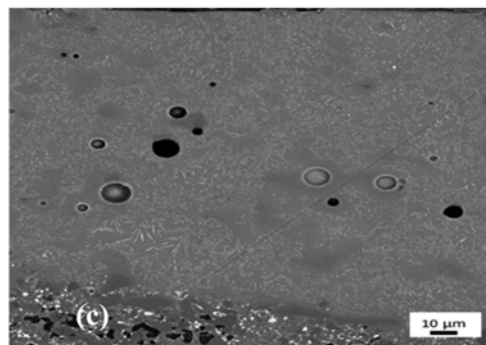
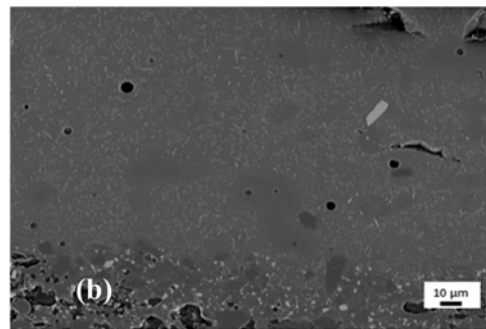
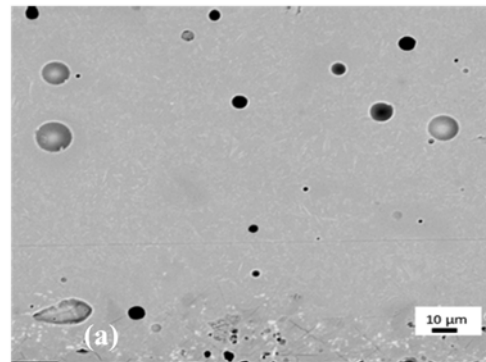


Fig. 6. SEM images of the glazes taken from cross section of the (a) Glaze R, (b) Glaze R50C, (c) Glaze R50B.

frit C was added, was determined to have increased. As for the second anticipation, the T softening value of the R20A glaze prepared using frit A decreased as it has been expected, while there was only a little decrease in the R50B glaze, the amount of the frit B had been increased.

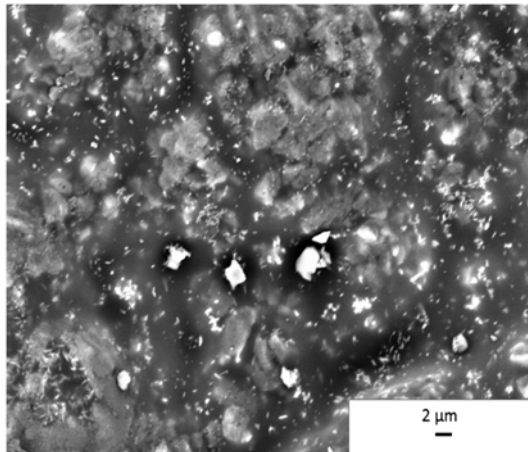
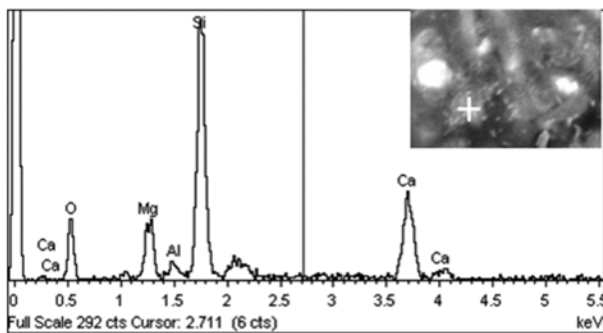
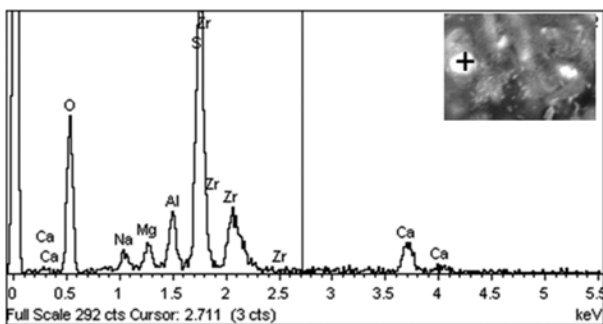
When the pinhole over the surface of the glaze was evaluated visually, it was determined that R50C and R50B glazes could be used as alternatives to the glaze R.

Fig. 5 shows the X-ray spectra collected from the surface of glazed tiles. Although there zircon crystals in the glazes of R and R20B, it was observed that diopside crystals had formed in the R50C glaze as an alternative to zircon. In addition, there were significantly more zircon crystals in R50C glaze, which was prepared according to our first anticipation, when compared to the other glazes.

Fig. 6 depicts the general microstructure of glazes

**Table 6.** L\*, a\*, b\*, glossness and defect value of glazed tiles.

| Glaze | L*    | a*   | b*   | 20 ° | 60 ° | 85 ° | Pinhole defect % |
|-------|-------|------|------|------|------|------|------------------|
| R     | 89,99 | 0,63 | 0,39 | 72   | 84   | 86   | 8                |
| R50B  | 90,00 | 0,62 | 0,19 | 71   | 84   | 86   | 3                |
| R50C  | 91,82 | 0,59 | 0,17 | 71   | 84   | 85   | 1                |

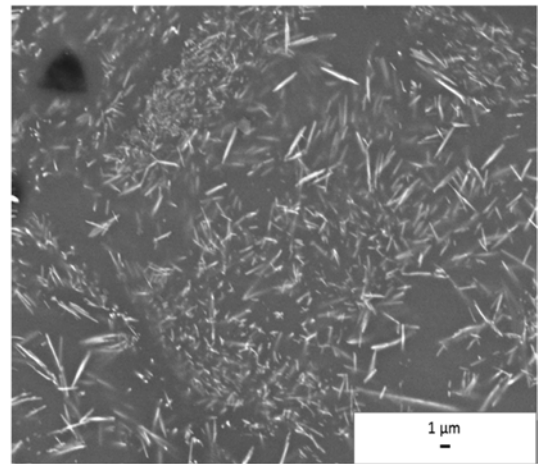
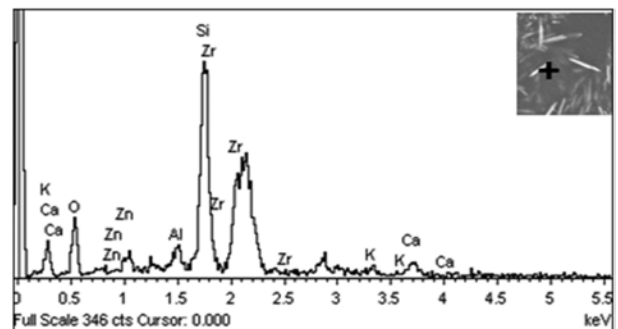
**Fig. 7.** SEM images of the glaze R taken from glaze surface.**Fig. 8.** EDX analyses of surface of R glaze by the point labeled (+).**Fig. 9.** EDX analyses of the surface of the R glaze by the point labeled (+).

from cross section. As was expected, there occurred fewer bubbles in the R50C glaze. Thus, it was quite easy to dispose of the bubbles in the glaze with the highest softening point. As to the R50B glaze, which was prepared according to our second anticipation, the bubbles were trapped in the system and so were prevented from reaching the surface. The bubbles were observed to have failed to advance towards the surface

in the glaze whose softening point had been reduced.

The results observed in microstructures were also confirmed by large-scale experiments of production. Table 6 presents the results of the production experiments with R-R50C and R50B glazes. While there was a pinhole defect in 8% of the tiles coated with the R glaze, this rate was reduced to only 1% in the tiles coated with the R50C glaze. The R50C glaze was also observed to have achieved the targeted properties in terms of glossiness and opacity.

Fig. 7 presents microstructure of the glaze R surface. EDX analyses of these surfaces are represented in Fig. 8 and 9. In addition to white zircon crystal (Fig. 8) the light-gray coloured structures that clustered in the microstructure of the R glaze do draw attention. According to the Fig. 9, these structures were assumed to have come together in order to form diopside crystals. However, because we could detect no diopside phases upon the XRD analysis, we assume that they failed to achieve a crystal structure and so left as an

**Fig. 10.** SEM images of the glaze R50C taken from glaze surface.**Fig. 11.** EDX analyses of the surface of the glaze R50C taken by the point labeled (+).

amorphous phase separated from matrix.

Although there appeared peaks with little severity in diopside crystals in the R50C glaze upon the XRD analysis, no crystal structures could be detected other than the zircon ones. Fig. 10 shows the microstructure of the glaze R50C surface. SEM photographs of the glass-ceramic glazes in which the backscattered electron technique enables registering compositional differences between glass and the crystals, where white coloured zircon crystals (Fig. 11) are observed immersed in a dark grey coloured glassy matrix.

The size of the majority of the homogeneously-distributed crystals vary between 0,5 and 1  $\mu\text{m}$ . They have a needle shape in a size varying between 0,3 and 0,5  $\mu\text{m}$ . The crystals occurring in the glaze whose softening point increased seem to have lacked enough time to grow.

### Conclusions

The present study suggests that the pinhole problem observed under industrial conditions could be solved rapidly with the help of simple thermal analysis techniques. The ratios of the frit can be adjusted in such a way as to increase the softening point by analysing crystallization and sintering behaviour of the frits added into the glaze by means of differential thermal analyses and the hot stage microscope respectively. The bubbles occurring in the glaze whose softening temperature had increased could be disposed of with ease and the system could be sintered afterwards. However, the crystals tend to fail to find enough time to grow once sintering and devitrification temperatures have been raised, thus the forming crystals

appear close to the wavelength of incident light. These crystals are really effective in light scattering and therefore cause a rise in opacity.

### Acknowledgments

The authors would like to thank Dr. Ender SUVACI, R&D Director Mr. Hidayet ÖZDEMİR and R&D Manager Mrs. Yesim BALTACI for their help and fruitful discussions throughout this study.

### References

1. I. Gutzow, J. Schmelzer, "The Vitreous State" (Heidelberg: Springer-Verlag Berlin, 1995).
2. C.R. Santos, T.L.B. Fontana, E. Uggioni, H.G. Riella, A.M. Bernardin, Conference Proceedings, February 2004, 189-193.
3. J.R. Taylor, A.C. Bull, "Ceramics Glaze Technology", (London: Pergamon Press, 1980).
4. W.D. Kingery, "Introduction to Ceramics", (New York: John & Sons, 1976).
5. R. A. Eppler, and D. R. Eppler, "Glazes and glass coatings", (the American Ceramic Society, 1998).
6. M. J. Romero, M. Rincon and A. Acosta, J. Eur. Ceram. Soc. [23] (2003) 1629-1635.
7. B.E. Yekta, P. Alizadeh and L. Rezazadeh, J. Eur. Ceram. Soc. [26] (2006) 3809-3812.
8. F.J. Torres, E. Sola and J. Alarcón, J. Eur. Ceram. Soc., [26] (2006) 2285-2292.
9. C. Siligardi, M.C. D'arrigo and C. Leonelli, International Ceramics Journal, (September 2002) 88-92.
10. J. Aparici and A. Moreno, in: The Proceedings of the Congress Qualicer, Castellón, Spain, 1994, 317-340.
11. Mingarro, C. F., Invited conference, in: The Proceedings of the Congress Qualicer, Castellón, Spain, March, 1994.